Probing effective nucleon masses with heavy-ion collisions

D. D. S. Coupland, M. Youngs, Z. Chajecki, W. G. Lynch, M. B. Tsang, Y. X. Zhang, M. A. Famiano, T. K. Ghosh, B. Giacherio, M. A. Kilburn, Jenny Lee, H. Liu, F. Lu, P. Morfouace, P. Russotto, A. Sanetullaev, R. H. Showalter, G. Verde, and J. Winkelbauer

Phys. Rev. C **94**, 011601 — Published 1 July 2016

DOI: 10.1103/PhysRevC.94.011601

Probing the Effective Nucleon Masses with Heavy Ion Collisions

D.D.S. Coupland,[1,2] M. Youngs,[1,2] Z. Chajecki,[1,5] W.G. Lynch,[1,2,3] M.B. Tsang,[1,2,3*] Y. X. Zhang,[3,4] M.A. Famiano,[5] T.K. Ghosh,[6] B. Giacherio,[5] M. A. Kilburn,[1,2] Jenny Lee,[1,2] H. Liu,[7] F. Lu,[3] P. Morfouace,[1] P. Russotto,[8] A. Sanetullaev,[1,2] R. H. Showalter,[1,2] G. Verde,[8] and J. Winkelbauer[1,2]

[1]*National Superconducting Cyclotron Laboratory, Michigan State University, East Lansing, MI 48824, USA*
[2]*Department of Physics and Astronomy, Michigan State University, East Lansing, MI 48824, USA*
[3]*Joint Institute of Nuclear Astrophysics, Michigan State University, East Lansing, MI 48824, USA*
[4]*China Institute of Atomic Energy, P.O. Box 275 (10), Beijing 102413, P.R. China*
[5]*Department of Physics, Western Michigan University, Kalamazoo, MI 49008, USA*
[6]*Variable Energy Cyclotron Centre, 1/AF Bidhannagar, Kolkata 700064, India*
[7]*Texas Advanced Computing Center, University of Texas, Austin, TX 78758, USA*
[8]*INFN, Sezione di Catania, I-95123 Catania, Italy*

(Dated: September 14, 2015)

It has been generally accepted that momentum dependent potentials for neutrons and protons at energies well away from the Fermi surface cause both to behave as if their inertial masses are effectively 70% of the vacuum values. This similarity in effective masses may no longer hold in dense neutron-rich regions within neutron stars, core-collapse supernovae, and nuclear collisions. There, differences in the momentum dependent symmetry potentials may cause neutron and proton effective masses to differ significantly. We investigate this effect by measuring the energy spectra of neutrons, protons and charged particles emitted in ^{112}Sn+^{112}Sn and ^{124}Sn+^{124}Sn collisions at E_{beam}/A= 50 and 120 MeV with precision sufficient to distinguish, in principle, between effective interactions with very different values of the neutron and proton effective masses. These data and model comparisons point the way towards future advances in our capabilities to understand the density and momentum dependence of the nuclear symmetry energy.

*Correspondence author: tsang@nscl.msu.edu

Inside a finite nucleus or nuclear matter, a nucleon experiences a strong, momentum-dependent interaction with its surrounding medium that leads to an apparent reduction of its inertial mass, described by the term "effective mass" or "k-mass"[1, 2]. Such effective masses provide a convenient description of the momentum dependencies of mean-field potentials that arise due to exchange and other non-localities, Lorentz properties of the nucleon-nucleon interaction, and higher-order terms [1, 3–11]. Deeply bound nuclear states [1] and nucleon elastic scattering optical potentials [12] in nearly symmetric matter, defined by equal neutron (ρ_n) and proton (ρ_p) densities, require nucleon effective masses that are reduced at saturation density ($\rho_0 \approx 2.7 \times 10^{14} g/cm^3$) to about ≈ 70% of the vacuum values. A major part of this effect stems from a reduction in the single nucleon level density required by the Pauli exclusion principle [9]. Similar conclusions were drawn from relativistic nucleus-nucleus collisions [13].

In neutron rich environments, however, many theories predict that the difference between the momentum dependence of the potentials felt by protons and neutrons will cause the neutron (m_n^*) and proton (m_p^*) effective masses to differ [1–11], i.e. $m_n^* \neq m_p^*$. This splitting of the nucleon effective masses increases with neutron asymmetry and density of the interacting medium. It strongly influences the symmetry energy [1–11], the nuclear Equation of State (EoS) [14], the magnitude of shell effects in nuclei far from stability [5, 7], the thermal properties of neutron-rich nuclei, core-collapse supernovae [14,15], neutron stars [16, 17], and neutron star cooling by neutrino emission [17]. Calculations using Landau-Fermi liquid theory [18] and the non-relativistic Brueckner-Hartree-Fock [6] theory have predicted that $m_n^* > m_p^*$ in neutron rich matter, while other calculations using relativistic mean field (RMF) theory and relativistic Dirac-Brueckner theory [4, 7] predict that $m_n^* < m_p^*$. A recent attempt to use experimental constraints on the magnitude and slope of the symmetry energy at ρ_0 to constrain the mass splitting somewhat preferred $m_n^* > m_p^*$ [19], as did optical model analyses of nucleon-nucleus elastic scattering [20]. However, uncertainties in the effective mass splitting and its density dependence remain large, especially for $\rho > \rho_0$, compelling efforts to constrain this density dependence.

Matter in the "participant" region formed in heavy ion central collisions by the overlap of neutron-rich projectiles and targets can be compressed and subsequently expand, reflecting properties of the EoS at $\rho > \rho_0$. Nuclear transport calculations predict that fast neutrons will predominantly come from the compressed participant region because of the more repulsive neutron potential and that they experience a higher acceleration for $m_n^* < m_p^*$, than do fast protons at the same momentum, resulting in an enhanced ratio of neutron over proton (n/p) spectra at high energies [3,10,21]. In contrast, calculations for $m_n^* > m_p^*$ predict that the effective masses enhance the acceleration of protons relative to neutrons resulting in a lower n/p spectral ratio [21]. These issues can only be explored with heavy ion collisions [21]. In this letter, we present the first measurements of n/p spectral ratios with sufficient precision to distinguish between the theoretically predicted n/p spectral ratios for different effective mass splitting [21,22].

We investigate these issues by measuring transverse neutron and proton spectra from central ^{124}Sn+^{124}Sn and ^{112}Sn+^{112}Sn collisions. The ^{124}Sn and ^{112}Sn beams were accelerated to E_{beam}/A = 50 and 120 MeV at the Coupled Cyclotron Facility and impinged upon 5 mg/cm^2 ^{112}Sn and ^{124}Sn foil targets at the National Superconducting Cyclotron Laboratory.

Hydrogen and helium isotopes were detected and isotopically resolved by six ΔE-E charged-particle telescopes from the Large Area Silicon Strip Array (LASSA) [23] placed 20 cm from the target. Each LASSA telescope consisted of a 500 μm double-sided ΔE silicon strip detector (DSSD) backed by an E detector consisting of four 6 cm thick CsI(Tl) crystals arranged in quadrants. These six telescopes spanned the polar angle range $23^\circ < \theta_{lab} < 57^\circ$ with a 0.9° angular resolution.

Neutrons were detected by the two walls of the MSU Large Area Neutron Array (LANA) [24], placed across the beam axis from LASSA at 5 m and 6 m from the reaction target. The LANA spanned polar angles of $15^\circ < \theta_{lab} < 58^\circ$ with an angular resolution of 0.8°-0.9°. Neutrons were distinguished from γ-rays by pulse shape discrimination and from charged particles by use of a charged-particle veto array of BC-408 plastic scintillator detectors placed between the target and the neutron walls. Neutron kinetic energies were determined by time of flight, measured with 1 ns resolution, using a start time supplied by an array of thin NE-110 plastic scintillators located 10 cm downstream from the target. The background from secondary scattering of neutrons from the floor and other materials was determined via shadow bar measurements.

In central collisions at this energy, most of the particles are direct participants in the reaction, forming a midrapidity region that is first compressed, then rebounds and expands, emitting nucleons and light clusters in the process. Nucleons and light clusters from the participant region were detected by the MSU Miniball

[25], an array of phoswich detectors that covered 70% of the lab frame solid angle in the chosen configuration. The Miniball primarily measured the multiplicity and transverse energy of charged particles emitted from this participant region, which is on average a monotonically decreasing function of impact parameter [26]. Gating on the highest 6% of the multiplicity distribution, we selected central reactions with impact parameters less than 3 fm, thereby ensuring that most $Z \leq 2$ particles detected in LASSA and LANA are participants in the collision.

To further ensure that light particles detected in LASSA and LANA are emitted from the participant region, an angular cut of $70^\circ < \theta_{CM} < 110^\circ$ is applied to select particles emitted in the transverse direction. Over this angular domain the center-of-mass energy spectra for these particles remains independent of angle [27]. The shapes and ratios of our experimental spectra are insensitive to variations of the experimental impact parameter range from $0 < b < 3fm$ to $0 < b < 6fm$. This observation is consistent with results from transport simulations [28].

Neutron and proton center-of-mass energy spectra, $\frac{dM_{n,124}}{dE_{CM}d\Omega_{CM}}$ and $\frac{dM_{p,124}}{dE_{CM}d\Omega_{CM}}$, from the ^{124}Sn+^{124}Sn reaction at E_{beam}/A = 50 MeV are shown as the solid points in the top and bottom left panels of Fig. 1. These spectra are normalized to provide the differential multiplicities of neutrons and protons, respectively. The single-neutron detection efficiency was evaluated using the SCINFULQMD Monte Carlo code [29], which calculates the efficiency of NE-213 scintillators to an estimated accuracy of 15%. Known systematic and statistical uncertainties in the spectra are smaller than the data points in this figure. As many transport models have difficulty reproducing the relative abundances of light isotopes produced as the system expands and disassembles, we determine the coalescence invariant (CI) neutron and proton spectra by combining the free nucleons with those bound in light isotopes with $1 < A < 5$. The solid points in the middle and right panels of Figure 1 indicate the corresponding neutron and proton CI spectra at E_{beam}/A = 50 and 120 MeV, respectively, which are constructed by adding the protons and neutrons in light clusters to the free nucleon spectra [29] as follows

$$\frac{dM_{n,CI}}{dE_{CM}d\Omega_{CM}} = \sum_{N,Z} N \cdot \frac{dM(N,Z)}{d(E/A)_{CM}d\Omega_{CM}}$$

$$\frac{dM_{p,CI}}{dE_{CM}d\Omega_{CM}} = \sum_{N,Z} Z \cdot \frac{dM(N,Z)}{d(E/A)_{CM}d\Omega_{CM}} \quad (1)$$

where $\frac{dM_{n,CI}}{dE_{CM}d\Omega_{CM}}$ and $\frac{dM_{p,CI}}{dE_{CM}d\Omega_{CM}}$ denote the coalescence invariant neutron and proton spectra, $\frac{dM(N,Z)}{d(E/A)_{CM}d\Omega_{CM}}$ denotes the measured differential multiplicity spectrum for fragments of charge and neutron numbers Z and N. The summation includes n, p, d, t, ^{3}He and ^{4}He.

While the free proton and neutron spectra were cleanly measured up to energies of E_{CM} =100 MeV, the upper limits in E_{CM}/A of our measured clusters are lower, reflecting their ranges in the 6 cm thick CsI(Tl) crystals of LASSA. The small contributions of $A \geq 3$ clusters that penetrate through LASSA can be neglected. However, non-negligible deuteron contributions to the coalescence invariant spectra beyond E_{CM} ≈ 55 MeV were extrapolated to higher energies via a coalescence approximation, i.e

$$\frac{dM_d}{d(E/A)_{CM}d\Omega_{CM}} = C \cdot \frac{dM_n}{dEd\Omega_{CM}} \cdot \frac{dM_p}{dEd\Omega_{CM}} \quad (2)$$

where C is a normalization factor determined by matching the product on the right to the measured deuteron spectrum [31]. The systematic uncertainty of this extrapolation to $E_{CM} > 55$ MeV is less than 1% and 2.5% at E_{beam}/A = 50 MeV and 120 MeV, respectively.

Due to the dynamical nature of nucleus-nucleus collisions, comparison of data to transport models is necessary. Recent studies indicate that n/p spectral ratios at high nucleon energies display high sensitivity to the effective mass splitting [21]. To illustrate this sensitivity, we compare our data to predictions from the ImQMD-Sky quantum molecular dynamics (QMD) transport model [21]. In this version of the QMD model, standard Skyrme interactions used to describe nuclear structure properties can be included in the nucleon potentials. Specifically, we focus on calculations that employ the SkM* and SLy4 Skyrme potentials, which have a similar slope of the symmetry energy with density (L) (compatible with Ref. [29]) but opposite mass splitting at saturation density as shown in Table I. At $\rho = \rho_0$ and $\delta = (\rho_n - \rho_p)/\rho_0 = 0.2$, the SkM* potential has $m_n^* > m_p^*$ with a fractional isovector mass correction $\delta K_I = m_n/m_n^* - m_p/m_p^* = -0.096$, while the SLy4 potential has $m_n^* < m_p^*$ with $\delta K_I = 0.062$. The calculations were performed at the impact parameter of 2 fm. Bound nuclei are identified by the proximity of nucleons to each other in position and momentum space in the final stages of the simulation.

Calculated free and CI nucleon spectra are shown in Figure 1. The solid lines and dashed lines correspond to calculations performed with the SLy4 and SkM* mean fields, respectively. The difference between the two calculations appears strongest for the calculated proton spectra, an effect that may reflect the interplay between

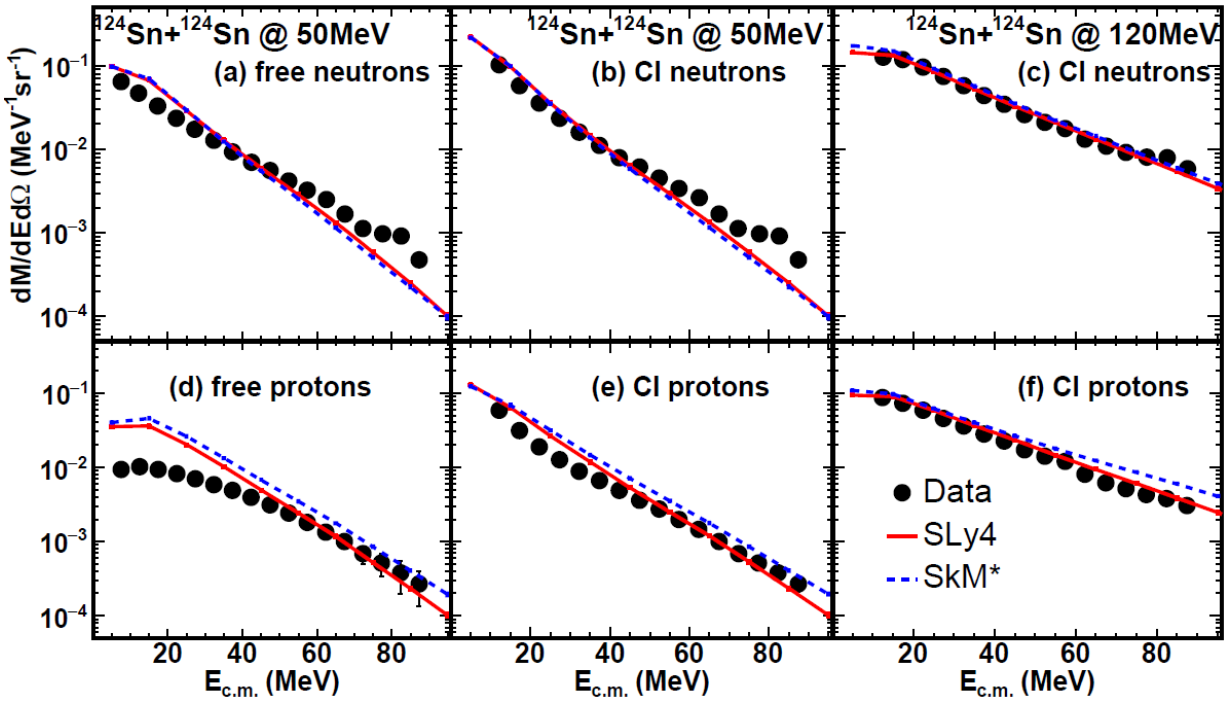

FIG. 1: (Color online) Free neutron (a) and free proton (d), and CI neutron (b) and CI proton (e) spectra from ^{124}Sn+^{124}Sn reaction at 50 MeV and CI neutron (c) and CI proton (f) spectra from ^{124}Sn+^{124}Sn reaction at E_{beam}/A=120 MeV (black data points) compared to ImQMD-Sky calculations (solid and dashed lines).

the symmetry energy and Coulomb dynamics [32], as well as differences in the isoscalar terms in the SLy4 and SkM* effective interactions, which can influence both neutron and proton spectra but cancel in the n/p spectral ratios. At these energies, the CI data and calculations are in better agreement than the free data and calculations. This reflects the fact that these calculations under-predict the yields of bound nuclei (especially ^{4}He), due in part to their under-predicting the binding energies of such well-bound nuclei; thus, nucleons in ^{4}He can be wrongly predicted to be emitted as free nucleons. The calculations over-predict the CI neutron and proton data at low energies and have a steeper energy dependence. The disagreement at E_{cm} < 20 MeV may be influenced by the neglect of fragments with Z≥3, which were not measured in this experiment. The discrepancies in the slope at E_{cm} > 40 MeV, however, suggests inaccuracies in the treatment of the isoscalar dynamics and the symmetric matter EoS that influences both n and p spectra. The amount of bound clusters that survives the expansion is less at higher energies making the theoretical inaccuracy in cluster production less problematic. The better agreement between data and calculations observed at E_{beam}/A = 120 MeV, facilitates stronger conclusions about the mass splitting at higher beam energies [21].

Sensitivity to the symmetry energy can be enhanced and isoscalar dynamics suppressed by dividing $\frac{dM_{n,CI}}{dE_{CM}d\Omega_{CM}}$ by $\frac{dM_{p,CI}}{dE_{CM}d\Omega_{CM}}$ for each reaction to obtain the n/p spectral ratio $R_{n/p}(CI)$.

$$R(n/p\,,CI,124) = \frac{\frac{dM_{n,CI}(124)}{dE_{CM}d\Omega_{CM}}}{\frac{dM_{p,CI}(124)}{dE_{CM}d\Omega_{CM}}} \qquad (3)$$

We further enhance effects due to the difference between neutron and proton effective masses by constructing the coalescence invariant double ratios

$$DR(n/p) = \frac{R(n/p,CI,124)}{R(n/p,CI,112)} \qquad (4)$$

as a function of E_{CM}. $R(n/p,CI,112)$ is obtained via an analogous expression involving the measured ^{112}Sn+^{112}Sn spectra. Like many observables, such as analyzing powers, the double ratio is chosen to minimize systematic uncertainties in order to measure a small effect reliably. In our work, the largest uncertainties lie in the detection efficiencies for both neutrons and charge particles for which the corrections are energy dependent and can exceed 15%. A second uncertainty concerns uncertainties in the energy calibrations or efficiencies for the charged particles. The double ratio cancels out both corrections.

Skyrme	S_0(MeV)	L (MeV)	m_{n^*}/m_n	m_{p^*}/m_p	δK_I
SLy4	32	46	0.68	0.71	0.062
SkM*	30	46	0.82	0.76	-0.096

TABLE I: Parameters of the Skyrme mean filed potentials for the calculations shown in Figs. 1 and 2. The effective mass for neutron and proton are obtained for isospin asymmetric nuclear matter with δ = 0.2.

Figure 2 shows the measured CI spectral double ratios DR(n/p) for both beam energies. There are systematic uncertainties (not shown in Figure 2) in DR(n/p) of about 10% at E_{beam}/A = 50 MeV and 15% at E_{beam}/A = 120 MeV stemming from the dependence of the neutron detection efficiencies on the charged particle and neutron scattering backgrounds in LANA. Previous double ratio data from Ref. [30], shown by green stars in the top panel, had a larger impact parameter cut at b < 5 fm. However, extending our data or calculations out to b < 6 fm does not change significantly measured or calculated [28] double ratios. The current data at E_{beam}/A =50 MeV have a factor of four smaller uncertainties and extend over a wider energy range than those of Ref. [30]. Where the two data overlap, they are within statistical and systematic uncertainties with Ref. [30], except the lowest two energy data point. Detailed comparisons of the neutron and proton data of the two experiments [34] indicate that the difference lies in the free neutron data, where hardware problems in the previous experiment should have included larger systematic corrections to the neutron spectrum.

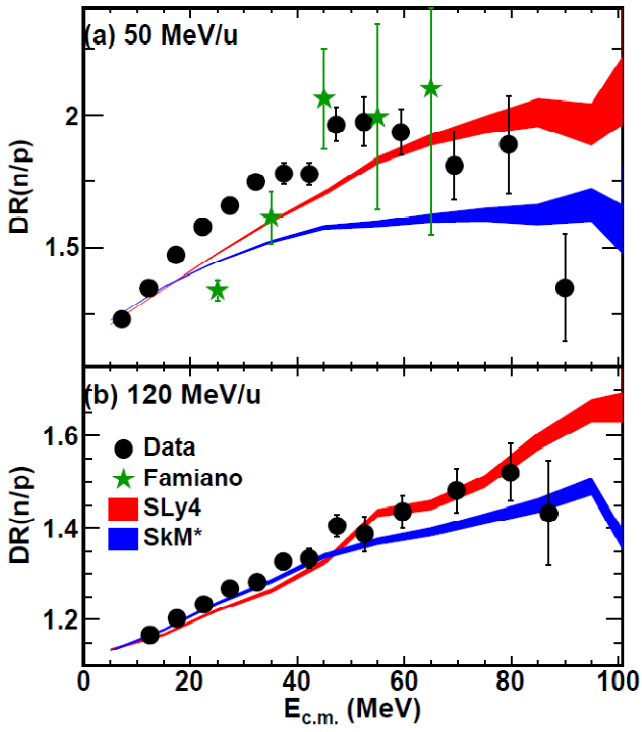

FIG. 2: (Color online) Neutron to proton double ratio (Eq. 3) for *Sn* + *Sn* collisions at E_{beam}/A=50 MeV (a) and 120 MeV (b).

Several transport calculations [11, 21, 22, 27, 28, 35, 36, 37, 40] have been used to calculate the n/p yield ratios for the experimental systems at E_{beam}/A = 50 MeV. Earlier attempts to extract information about the mass splitting were unsuccessful due to insufficient statistical accuracy [22]. The case of IBUU codes is more complex. Early version of IBUU [35] compared better to the present data and that of ref. [30], but later versions such as IBUU04 [37] and IBUU11 [40] significantly under-predict the measured DR, providing values close to the insensitivity value of 1.2=(148/100)/(124/100) defined as the ratio of total neutron to total proton numbers of the measured ^{124}Sn+^{124}Sn and ^{112}Sn+^{112}Sn systems. Other transport models including pBUU [39] and Stochastic Mean Field (SMF) [11] codes predict larger n/p ratios that are more comparable to the data. The inability to reproduce the magnitude of measured double ratios in IBUU transport model [37, 40] led to the suggestion that reproduction of observed double ratios may require explicit treatment of tensor and short-range correlations [38,40]. It is an interesting idea. However the implementation should be done consistently and tested in different models.

At higher incident energy, E_{beam}/A=120 MeV, the calculation describes the nucleon spectra fairly well. Furthermore, at high nucleon energies (E_{cm}>60 MeV), the ImQMD_sky calculations of ref. [21] showed the greatest sensitivity to the effective mass splitting, the SLy4 calculations (upper curve) lie close to the data while the SkM* calculations (lower curve) lie below the data. At E_{beam}/A =50 MeV, there is no agreement between the data and calculations. The disagreement reflects the inability of the calculations to describe high energy neutron data in Figure 1. Theoretical analyses, however, indicate that n/p yield ratios (as well as other observables) are somewhat sensitive to other transport properties such as the isoscalar effective mass [32], which may have to be constrained better in order to accurately determine the effective mass splitting. In the absence of such results and excepting the high energy points, which trend somewhat downwards in the double ratio, these comparisons indicate the effective mass splitting is closer to that predicted by the SLy4 interactions but the uncertainties are large.

In summary, we have presented new neutron/proton spectral double-ratio data from central ^{124}Sn+^{124}Sn and ^{112}Sn+^{112}Sn collisions at two widely separated beam energies. These measurements provide an increase in accuracy and kinetic energy range compared to previous data at E_{beam}/A = 50 MeV, and provide new data at the previously unmeasured beam energy of E_{beam}/A = 120 MeV.

We acknowledge the support of the NSCL beam physics and Coupled-Cyclotron Facility operations staff, Michigan State University and the Texas Advanced Computing Center at University of Texas, Austin. This material is based upon work supported in part by the National Science Foundation under Grant Nos. PHY 1102511, PHY 1510971 and PHY-1430152.

[1] C. Mahaux, P. F. Bortignon, R. A. Broglia, and C. H. Dasso, Phys. Reports **120**, 1 (1985).
[2] E. N. E. van Dalen, C. Fuchs, and A. Faessler, Phys. Rev. Lett. **95**, 022302 (2005).
[3] V. Giordano, M. Colonna, M. Di Toro, V. Greco, and J. Rizzo, Phys. Rev. C **81**, 044611 (2010).
[4] B. Liu, V. Greco, V. Baran, M. Colonna, and M. Di Toro, Phys. Rev. C **65**, 045201 (2002).
[5] J. Dobaczewski, Acta Physica Polonica B **30**, 1647 (1999).
[6] W. Zuo, A. Lejeune, U. Lombardo, and J. F. Mathiot, The European Physical Journal A **14**, 469 (2002).
[7] F. Hofmann, C. M. Keil, and H. Lenske, Phys. Rev. C **64**, 034314 (2001).
[8] C. Fuchs and H.H. Wolter, The European Physical Journal A **30**, 5 (2006).
[9] J. Blaizot and B. Friman, Nucl.Phys. **A372**, 69 (1981).
[10] J. Rizzo, M. Colonna, and M. Di Toro, Phys.Rev. **C72**, 064609 (2005).
[11] H. H. Wolter, M. Zielinska-Pfabe, P. Decowski, M. Colonna, R. Bougault and A. Chbihi, EPJ Web of Conf. 66, 03097 (2014).
[12] E. Bauge, J. P. Delaroche, and M. Girod, Phys. Rev. C **63**, 024607 (2001).
[13] P. Danielewicz, Nucl. Phys. A **673**, 375 (2000).
[14] Sanjay Reddy, Madappa Prakash, James M. Lattimer, and Jose A. Pons, Phys. Rev. C 59, 2888 (1999).
[15] H.A. Bethe, Rev. Mod. Phys. 62, 801 (1990).
[16] J. Pons, S. Reddy, M. Prakash, J. Lattimer, and J. Miralles, Astrophys. J. **513**, 780 (1999).
[17] M. Baldo, G. F. Burgio, H.-J. Schulze, and G. Taranto, Phys. Rev. C **89**, 048801 (2014).
[18] O. Sjoberg, Nucl. Phys. A **265**, 511 (1976).
[19] B.-A. Li and X. Han, Phys. Lett. B **727**, 276 (2013), ISSN 0370-2693.
[20] X.-H. Li, W.-J. Guo, B.-A. Li, L.-W. Chen, F. J. Fattoyev, and W. G. Newton, Physics Letters B **743**, 408 (2015).
[21] Y. Zhang, M. B. Tsang, Z. Li, and H. Liu, Phys. Lett. B **732**, 186 (2014).
[22] W.-J. Xie, J. Su, L. Zhu, and F.-S. Zhang, Phys. Rev. C **88**, 061601 (2013).
[23] B. Davin, R. T. de Souza, R. Yanez, Y. Larochelle, R. Alfaro, H. Xu, A. Alexander, K. Bastin, L. Beaulieu,J. Dorsett, et al., Nucl. Instrum. Meth. A **473**, 302 (2001).
[24] P. D. Zecher, A. Galonsky, J. J. Kruse, S. J. Gaff, J. Ottarson, J. Wang, F. Deak, A. Horvath, A. Kiss, Z. Seres, et al., Nucl. Instrum. Meth. A **401**, 329 (1997).
[25] R. T. D. Souza, N. Carlin, Y. D. Kim, J. Ottarson, L. Phair, D. R. Bowman, C. K. Gelbke, W. G. Gong, W. G. Lynch, R. A. Pelak, et al., Nucl. Instrum. Meth. A **295**, 109 (1990).
[26] C. Cavata, M. Demoulins, J. Gosset, M.-C. Lemaire, D. L'Hˆote, J. Poitou, and O. Valette, Phys. Rev. C **42**, 1760 (1990).
[27] M.Youngs, NSCL/MSU PhD. Thesis (2013), https://groups.nscl.msu.edu/nscl_library/Thesis/Youngs,Michael.pdf
[28] Y. Zhang, P. Danielewicz, Z. Li, H. Liu, F. Lu, et al., Phys. Rev. C **85**, 024602 (2012).
[29] D. Satoh, T. Sato, N. Shigyo, and K. Ishibashi, Tech. Rep., Japan Atomic Energy Agency (2006), jAEAData/Code 2006-023.
[30] M. A. Famiano, T. Liu, W. G. Lynch, M. Mocko, A. M. Rogers, M. B. Tsang, M. S. Wallace, R. J. Charity, S. Komarov, D. G. Sarantites, et al., Phys. Rev. Lett. **97**, 052701 (2006).
[31] Z. Chajecki, M. Youngs, D. Coupland, W. Lynch, M. Tsang, et al., ArXiv:1402.5216 (2014).
[32] Y. Zhang, M. Tsang, and Z. Li, Phys. Lett. B **749**, 262 (2015).
[33] M. B. Tsang, J. R. Stone, F. Camera, P. Danielewicz, R. Gandolfi, K. Hebeler, C. J. Horowitz, J. Lee, W. G. Lynch, Z. Kohley, et al., Phys. Rev. C **86**, 015803 (2012).
[34] M. Famiano (2013), private communication.
[35] B.-A. Li, C. M. Ko, and Z. Ren, Phys. Rev. Lett. **78**, 1644 (1997).
[36] Y. Zhang, P. Danielewicz, M. Famiano, Z. Li, W. Lynch, and M. Tsang, Phys. Lett. B **664**, 145 (2008).
[37] B.-A. Li, L.-W. Chen, G.-C. Yong, and W. Zuo, Phys. Lett. B **634**, 378 (2006).
[38] Or Hen, Bao-An Li, Wen-Jun Guo, L.B. Weinstein, Eli Piasetzky, Phys.Rev. C91 (2015) 025803.
[39] P. Danielewicz, Nucl. Phys. A 673, 375 (2000).
[40] Hai-Yun Kong, Yin Xia, Jun Xu, Lie-Wen Chen, Bao-An Li, and Yu-Gang Ma Phys. Rev. C 91, 047601 (2015).